

IMPROVEMENT OF THE MEASUREMENT CHAIN LINKING THE FARAD TO THE OHM AT LNE

Ralph, Sindjui^{1,a}; Olivier, Thévenot¹; Pierre, Gournay²; François, Piquemal¹; Gael, Thuillier¹; Saïf, Khan¹ et Olivier, Séron¹

¹Laboratoire National de Métrologie et d'Essais (LNE), 29 avenue Roger Hennequin 78197 Trappes Cedex, France
²Bureau International des Poids et Mesures (BIPM), Pavillon de Breteuil, 12 bis Grande Rue 92310 Sèvres, France

Résumé. Cet article présente l'amélioration de la chaîne de mesure du LNE permettant la réalisation de l'ohm à partir du farad. Celle-ci est mise en œuvre afin de déterminer le quantum de résistance R_K issu de l'effet Hall quantique à partir d'un condensateur calculable permettant la réalisation du farad dans le SI. Elle comporte différents ponts d'impédances coaxiaux en deux et quatre paires de bornes dont l'élément central est un transformateur étalon. Nous décrivons dans cet article une nouvelle génération d'autotransformateurs étalons double étage conçus et caractérisés dans le but d'améliorer la chaîne de mesure d'impédance du LNE et réduire l'incertitude globale sur la détermination de R_K à une valeur proche de 10^{-8} .

1 Introduction

As a part of the redefinition of the International System of Units (SI) based on fundamental constants [1], the determination of the von Klitzing constant R_K with an uncertainty of one part in 10^8 presents some interest.

Indeed, the comparison of the SI values of R_K obtained from direct determinations with other accurate measurements of h/e^2 serves as a relevant test of validity of the quantum Hall effect theory predicting the relation $R_K = h/e^2$, a decisive issue within the context of the new SI (with h the planck constant and e the charge of the electron).

Direct measurement of R_K is obtained by linking the ohm produced from the quantum Hall effect to the farad achieved from a Thompson-Lampard calculable capacitor [2,3], using a dedicated high precision measurement chain. At LNE, the last determination of R_K was conducted in 2000 with an uncertainty of 5 parts in 10^8 [2]. In order to reach the target uncertainty of one part in 10^8 , the LNE needs to build a new calculable capacitor and to improve the associated measuring chain. This last point involves in particular the design and the characterization of new standard autotransformers which design and calibration is described below.

2 Measurement chain

Several coaxial impedance comparison bridges are used for the determination of R_K . The overall view of the successive measurements is shown in Figure 1. The measurements are carried out at 3 angular frequencies $\omega = 2500$ rad/s, 5000 rad/s and $10\,000$ rad/s.

First, a 1 pF capacitor is compared to the Thompson-Lampard calculable capacitor with a two terminal-pair bridge, the ratio of which being adapted to the

capacitance variation produced by the calculable capacitor.

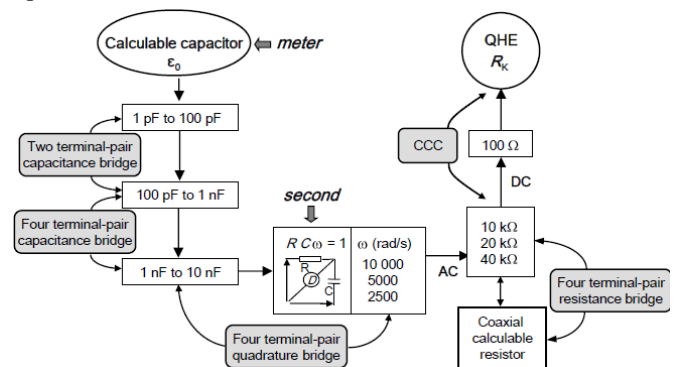


Figure 1. Measurement chain of the determination of R_K

Then two 10:-1 coaxial ratio bridges (two and four terminal-pair) are used successively to link two 10 nF capacitors (homemade invar plates in vacuum capacitors) to the calculable capacitor. The 1 nF transfer standard is a nitrogen sealed capacitor in oil bath while the 10 and 100 pF transfer standards are thermoregulated fused silica capacitors (Andeen-Hagerling capacitors). Next, a quadrature bridge is used to compare the impedances of the 10 nF capacitors to that of pair of resistors. Three couples of resistors are used with values of 40, 20 and 10 k Ω , the bridge being balanced for the three angular frequencies 2500 rad/s, 5000 rad/s and 10 000 rad/s, respectively. The quadrature bridge is a 1:-1 four-terminal-pair bridge derived from the classical models described by Cutkosky [4] and Kibble [5]. Finally, taking into account their frequency dependence, by means of AC/DC calculable resistance standards, these resistances are compared to the quantum Hall resistance standard in DC leading to a SI value of the von Klitzing constant.

^a ralphariel.sindjui@lne.fr

This comparison is made using a Cryogenic Current Comparator (CCC) based resistance bridge.

Details of the implementation of these bridges are given in the reference [2]. Figure 2 hereafter shows the principle of a coaxial AC bridge for impedance comparison.

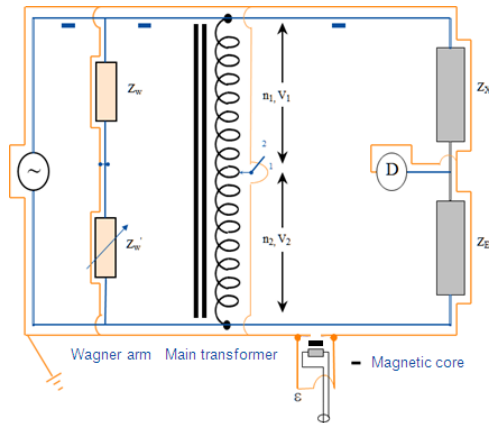


Figure 2. Principle of a coaxial AC bridge with Z_X and Z_E the impedances in comparison, D the detector, ϵ the injection voltage. The Wagner arm is used to overcome the effect of the leakage impedances. The ratio of the bridge is ensured by the main transformer.

The key elements used in the 10:-1 ratio bridges are standard transformers. During the last determination of R_K , the more penalizing uncertainty components associated to the measuring chain are following: the ratios of the AC bridges ($1,5 \cdot 10^{-8}$), the voltage effect of the capacitors 10 pF, 100 pF, 1000 pF ($1 \cdot 10^{-8}$) and the frequency dependence of the transfer resistors ($1,5 \cdot 10^{-8}$). A large amount of work has already been carried out to minimize the effect of the frequency dependence. In order to reduce the uncertainties associated to these bridges, a new generation of two-stage autotransformers has been developed and calibrated.

3 Two-stage autotransformer standard

3.1 Principle

An autotransformer is a transformer in which the secondary winding is a part of the primary one. Compared to a traditional transformer, it allows one to decrease the number of windings and avoids potential fluctuations between primary and secondary coils.

Two-stage autotransformers are currently used to provide standard ratios [5]. The primary winding of such a device is composed of two windings wound on two separate toroidal magnetic cores as shown on Figure 3. The magnetizing winding, is wound on core 1, while the metrological winding, is wound around both the magnetic cores 1 and 2. Since the metrological stage acts mainly to compensate the flux leakages and the magnetic losses in the magnetizing core, its section doesn't need to be as large as the magnetizing one. The metrological winding is divided into sections which allow one to define the bridge ratio.

Magnetizing and metrological windings have the same number of turns and are supplied by the same

voltage source. This leads to a very low current in the metrological winding intended to provide the standard voltages. This induces a significant decrease of the effects of the leakage inductances and resistances which would exist in a single stage autotransformer. Therefore, the ratio corrections may be reduced by a factor of about 10^3 compared to a single stage autotransformer, leading to a ratio correction value below 10^{-7} at 1 kHz.

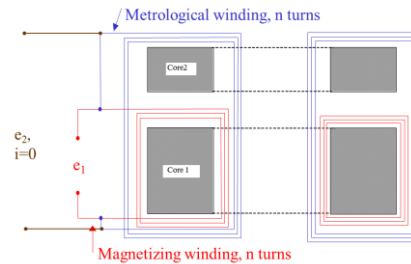


Figure 3. Sectional view of a two-stage autotransformer

3.2 Magnetic core

The magnetic cores are made of Nanophy® which has a very high permeability ($\mu_r > 100\,000$ at 1 kHz) and a saturation flux density of 1.25 T. They consist of a nonconductive thin strip (about 20 μm) tightly wound into a spiral which allows to reduce the influence of Eddy currents while maintaining an important total flux through the section of the core. The autotransformer is designed to work at voltages up to 240 V for frequencies between 400 and 1600 Hz. Core sections are 19.5 cm^2 for the magnetizing one and 4.5 cm^2 for the metrological one.

3.3 Windings

Magnetizing and metrological windings have 240 turns. The magnetizing winding is made with enameled copper wire. Two guides (Figure 5 (a)) have been designed to obtain an uniform winding. An “anti-progression” turn has been added to decrease the effect of a disturbance due to a magnetic field perpendicular to the toroidal section [5].

The metrological winding has been wound using a modified “Ayrton-Perry” method described in [5]. This method permits to decrease significantly the self-capacitance of the winding and to make it insensitive to external magnetic fields. The winding consists of twelve sections of twenty turns each connected in series. They are made with three ribbons of four wires superimposed and separated by an insulator (Teflon). The potential allocation of the twelve wires has been chosen to minimize the effect of the inter-sections capacitances. Figure 4 shows the progression of application of the turns.

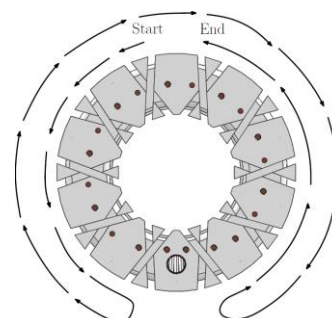


Figure 4. Progression of application of the turns using a modified “Ayrton-Perry” method

3.4 Electric and magnetic screens

Electric screen (Figure 5 (b)) and magnetic screen (Figure 5 (d)) are placed between the magnetizing and metrological windings allowing, for the first, to eliminate capacitive currents between windings, and for the second, to reduce the magnetic leakage of the magnetizing stage. The assembly is placed in a second magnetic shield (Figure 5 (c)) to protect the autotransformer against external electromagnetic fields.

Electric screen is made of copper and magnetic screens are made of Mumetal®.

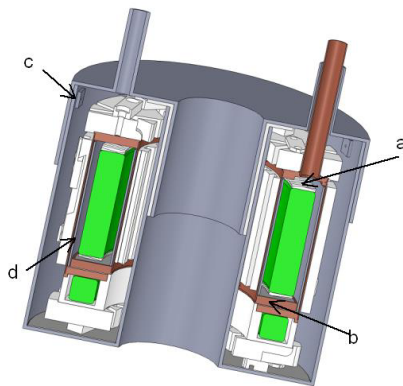


Figure 5. Sectional overview of the autotransformer

3.5 Connectors

The magnetizing stage is accessible by UHF connectors on the rear and the twelve sections (metrological stage) are accessible by BPO connectors on the front of the enclosing box as shown on Figure 6. Some of them were doubled to ensure the geometry’s consistency of the measuring loop during calibration.

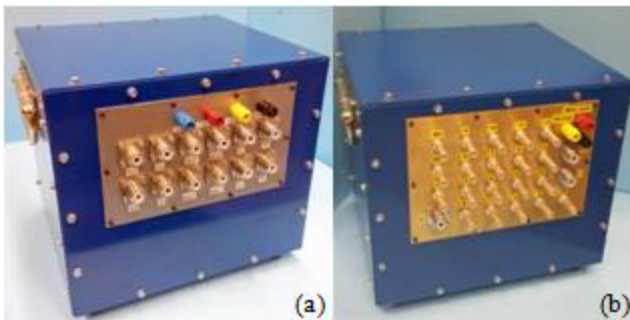


Figure 6. Final assembly of the standard two-stage autotransformer: (a) the rear, (b) the front

4 Calibration

The calibration is performed using the bootstrap method described in [5], slightly modified. It consists in successively comparing the terminal voltage of each section to a fixed voltage provided by a calibrating transformer. The voltage delivered by the calibrating transformer must be stable for the duration of the

measurements and independent of the working potential relative to the ground potential. A dedicated two-stage calibrating transformer of ratios 1:11 or 1:12 (depending on the calibration configuration) was constructed for this purpose. The comparison is performed with no current in the detection loop. Balance is achieved by means of an injection transformer associated to a generator of adjustable voltage in phase and quadrature. The injection is made on the metrological stage of the calibrating transformer. The detection of the balance is performed using a detection transformer associated with a lock-in amplifier.

By this method, relative uncertainties on the ratio corrections can be reduced at a level down to a few parts in 10⁹ or better. Figure 7 shows the calibration bridge used for the characterization of the autotransformer.

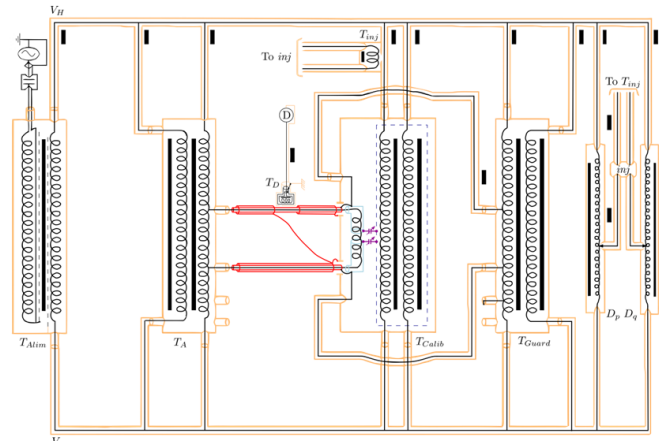


Figure 7. Calibration bridge with T_{Alim} the supply transformer, T_A the transformer under calibration, T_D the detection transformer, T_{inj} the injection transformer, T_{Calib} the calibrating transformer, T_{Guard} the guarding transformer, D_p and D_q the inductive voltage dividers

5 Results

With this new generation of standard autotransformers, the corrections have been decreased compared to the previous autotransformer used during the last determination of R_K . Those corrections have been determined with an uncertainty of about $1 \cdot 10^{-9}$ from 400 Hz to 1600 Hz for voltages ranging from 10 to 200 V. Hereafter are presented the corrections measured for the four frequencies at which the device is used.

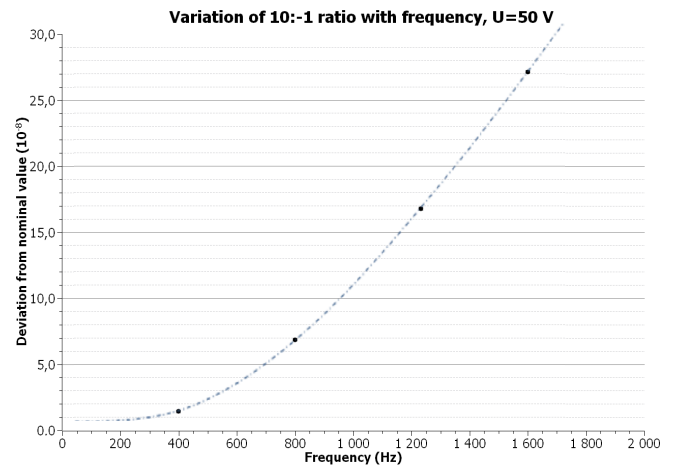


Figure 8. Variation of 10:-1 ratio with frequency at 50 V. The quadratic behavior of the correction with frequency is explained in [5]

The voltage behavior has also been studied and no deviation larger than 2.10^{-9} are observed between 10 V and 200 V from 400 Hz to 1600 Hz instead of 3.10^{-8} between 10 V and 100 V for the last generation.

Figure 9 shows the variation of the correction with the voltage at 800 Hz.

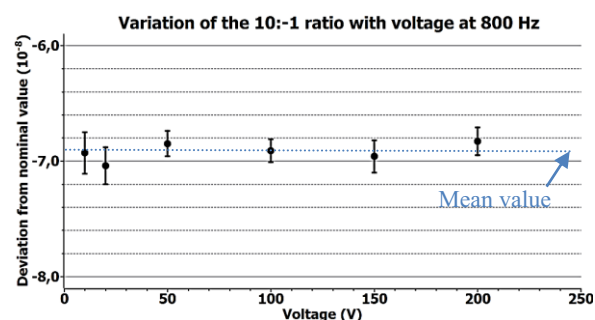


Figure 9. Variation of 10:-1 ratio with voltage at 800 Hz

6 Conclusion

The design and construction of the standard two-stage autotransformer is now completed. The corrections have been decreased by a factor of three compared to the previous autotransformer at 1600 Hz and are known with an uncertainty of about 1.10^{-9} from 400 Hz to 1600 Hz for voltages varying from 10 V to 200 V. The implementation of this autotransformer in the capacitance bridges used in the R_K measuring chain will reduce the contribution of the standard ratio uncertainty on the global uncertainty budget from 15 parts to 5 parts in 10^9 . This device is also used in the traceability chain implemented for the realization of the farad from the DC quantum Hall effect.

Furthermore; this new standard two-stage autotransformer could be used to determine the frequency behavior of the transfer resistances and the voltage effect of the transfer capacitors 10 pF, 100 pF, 1000 pF in order to reduce the associated uncertainty components.

References

1. Resolution 1 of the 24th meeting of the CGPM, BIPM Web site, <http://www.bipm.org/eu/CGPM/db/24/1/,2011>.
2. G. Trapon, O. Thévenot, J.C. Lacueille, W. Poirier, "Determination of the von Klitzing constant R_K in terms of the BNM calculable capacitor – fifteen years of investigations", *Metrologia*, 40, Iss. 4, 159-171 (2003).
3. P.Gournay, O.Thevenot, L.Dupont, J.M. David, F.Piquemal, "Toward a determination of the fine structure constant at LNE by means of a new

- Thompson-Lampard calculable capacitor", *Can. J. of Physics*, **Vol. 89**, n°1, 169, 2011
4. D. Cutkosky, "Techniques for comparing Four-Terminal-Pair admittance standards", *Journal of Research of the NBS*, **Vol. 74C**, No 3 and 4, p.63, (1970).
 5. B.P. Kibble, G.H. Rayner, "Coaxial AC Bridges", *Ed. A. E. Bailey*, (1984).